Supporting Information

Järvinen and Ruoslahti 10.1073/pnas.1016233107

SI Materials and Methods

Peptide Synthesis. Peptides were synthesized with an automated peptide synthesizer by using standard solid-phase fluorenylmethoxycarbonyl chemistry (1). During synthesis, the peptides were labeled with fluorescein using an amino-hexanoic acid spacer as described previously (1).

Primers and Decorin Cloning. The following primers were synthesized to amplify full-length human decorin cDNA from pGEM1–PG40 cloning vector (2) and to clone a Kozak sequence to the N terminus and EcoRI and SalI restriction sites and His tag into the C terminus of the decorin: 5′-ACGT GGATCCGGACCGTTTCAACAGAGAGGCTTATTTGACTT0054ATGCTAGA-3′ and 5′-ATCCGCTCGAGTTAGTGATGGTGATGGTGATGCGAGCTGCCGCGCGGCACCAGGTCG ACGAATTCCGAGCCCTTATAGTTTCCGAGTTGAATGGCAGA-3′. The resulting PCR product was then subcloned into mammalian expression vector pcDNA3.1/myc-his-C (Invitrogen). The peptides were cloned between the C terminus of the decorin and the His tag (Fig. 1) using EcoRI and SalI restriction sites regenerated by PCR allowing the following primers to anneal together: CAR, 5′-AATTTTGTGCA CGTTCGAAGAACAAAGATTGCG-3′ and 5′-TCGACGCAATCTTTGTTCTTCGAACG TGCACAA-3′; and *m*CAR, 5′-AATTTTGTGCGCGCAGTCGAACAATAAGGATTGCG-3′ and 5′- TCGACGTTAGCAATCCT TATTGTTCGACTGCACAA-3′. Human serum albumin (HSA) modified with CAR homing peptide was cloned by replacing the decorin cDNA with HSA cDNA (3) in the expression vector. A map of the extended C terminus of the decorin fusion proteins is shown in Fig. 1.

Production of Recombinant Proteins. The decorin and HSA constructs were expressed in 293-F cells using the FreeStyle 293 expression system from Invitrogen, according to the manufacturer's instructions. The cells were cultured for 48 h and the decorins and HSA were isolated from the media on Ni-NTA agarose beads (Qiagen) using 5 mL of beads per 500 mL of media. After an overnight incubation at +4 °C, the beads were washed with PBS, and decorin or HSA was eluted with PBS containing 300 mM imidazole, dialyzed against PBS, and stored at −80 °C.

Characterization of Recombinant Decorins. Recombinant decorins and CAR–HSA were analyzed on SDS/PAGE on 4–20% acrylamide gradient gels. The gels were either stained with Coomassie Blue or used to transfer the proteins to PVDF membrane, and immunoblots were performed with monoclonal anti–6-histidine tag antibody (1:1,000, clone 18184; Novus Biologicals) and goat antimouse IgG–HRP (diluted 1:25,000; Bio-Rad) and then developed using ECL plus chemiluminescence reagent (Amersham Biosciences), according to the manufacturer's instructions.

For mass spectrometry analysis, proteins were separated on 10% SDS/PAGE. Protein bands were detected by silver staining, extracted, and subjected to in-gel trypsin digestion and peptide mass fingerprinting in MALDI-TOF.

Protein folding was examined by differential scanning calorimetry using N-DSC II differential calorimeter (Calorimetry Sciences) at a scanning rate of 1 °C/min under 3.0 atm of pressure. Protein samples were dialyzed against PBS and the analyses were carried out at 1.0 mg/mL of protein.

Chondroitinase Treatment of Recombinant Decorins. The recombinant decorins were digested with chondroitinase ABC (Sigma-Aldrich) in chondroitinase buffer (0.3 M NaCl, 10 mM Tris, pH 7.4) containing protease inhibitors as described elsewhere (4–6. Briefly, chondroitinase ABC was added at 0.8 unit/mg of recombinant protein, the samples we incubated at +37 °C for 1 h and examined by SDS/PAGE.

Cell Proliferation and Cell Binding Assays. Chinese hamster ovary cells (CHO-K) were obtained from the American Type Culture Collection. The pgsA-745 mutant cell line, derived from CHO-K and defective in glycosaminoglycan synthesis (7), was kindly provided by Dr. J. Esko (University of California at San Diego, La Jolla, CA). Cells were maintained in α-MEM and Earle's salt supplemented with 10% FBS, 100 μg/mL streptomycin sulfate, 100 U/mL of penicillin G, and 292 μg/mL L-glutamine (Invitrogen).

The effect of decorin preparations on CHO-K cell proliferation was determined as described previously (8, 9). The cells were grown either in medium containing dialyzed FBS (Pierce) or in medium supplemented only with TGF-β1, -β2 or -β3 (7.5 ng/mL, Biovision). The cells were plated in duplicate at a density of 1×10^4 cells per well in 24-well plates and cultured in 1 mL of culture medium. Half of the medium was replaced daily with fresh medium containing recombinant decorins or HSA as well as TGF-β1/-β2/-β3 (7.5 ng/mL). Cells were collected by trypsinization, washed, and resuspended in 1 mL of PBS containing 2 μg/mL of propidium iodide (PI) and 20,000 CountBright counting beads (Invitrogen), and analyzed by counting viable cells in FACS. Cell number was also determined by hemocytometer.

To study decorin peptide binding and internalization, CHO-K and pgsA-745 cells seeded on plastic coverslips were incubated with different decorins and peptide for 4–72 h, washed three times with PBS, and fixed with 4% paraformaldehyde for 20 min at room temperature (10). After several washes with PBS, the primary antibodies against human decorin and 6-histidine were applied on slides for 1 h at room temperature, and the primary antibodies were detected with Alexa Fluor 488 anti-mouse and anti-rabbit IgGs (1:1,000 and 1:3,000, Invitrogen). After several washes with PBS, the nuclei were visualized by staining with DAPI, and the slides were mounted with ProLong Gold antifade reagent (Invitrogen). The images were acquired using Olympus IX81 inverted and Olympus Fluoview FV1000 confocal microscopes. *Z*-stack images were taken by confocal microscope every 1 μm through the cells.

Histology. Wound tissues were isolated, bisected, fixed overnight in 10% buffered zinc formalin (Statlab Medical Products), dehydrated, and embedded in paraffin. Longitudinal sections (6 μm) from the middle of the wound were stained with hematoxylin/eosin, picrosirius red (Sirius red F3BA 0.1% solution in saturated aqueous picric acid) (Sigma-Aldrich) or using the Masson trichrome procedure, or processed for immunohistochemistry. Two sections from the middle of wounds were quantitatively evaluated, and the average of the two values was used in the analysis. The length of hyperproliferative epidermis and size of the wound tissue were determined from the Masson trichrome stained tissue sections.

Quantitative Analysis of Histochemical and Immunostaining Stainings. Image analysis, quantification of histological parameters, and immunohistochemistry were done using Spectrum digital pathology system (Aperio Technologies) as described previously elsewhere (11). Briefly, all slides were scanned at an absolute magnification of 400× [resolution of 0.25 μm/pixel (100,000 pixel/in)] using the Aperio ScanScope CS and XT systems (Aperio Technologies)

(11). The background illumination levels were calibrated using a prescan procedure. Slides were viewed and analyzed with the ImageScope viewer. The area of interest was recorded manually for each wound. The Spectrum Analysis algorithm package and Image Scope analysis software (version 9; Aperio Technologies) were applied to quantify the area or the length of the marked area and the immunohistochemical signal. For the quantification of immunohistochemistry, the software separates the signal from the chromogen and hematoxylin by a color deconvolution method (11). Each stain (6-histidine tag, CTGF/CCN2, decorin, αSMA, F4/80, MPO) was individually calibrated and the average RGB optical density vectors were recorded (11). The algorithms calculate the area of positive staining (expressed as a percentage of negative (−), weak (1+), medium (2+), and strong (3+) positive staining and the average positive intensity (optical density).

Immunohistochemistry. Frozen sections were fixed in acetone for 10 min and preincubated with 0.5% blocking reagent for 1 h (NEN Life Sciences). Formalin fixed, paraffin-embedded tissue sections were deparaffinized, incubated with the blocking reagent, and endogenous peroxidase activity was suppressed with hydrogen peroxide. Tissue sections were incubated with the primary antibody overnight at 4 °C. After washing, bound primary antibodies were detected with appropriate secondary antibodies labeled with peroxidase or FITC. Each staining experiment included slides treated with species-matched immunoglobulins as negative controls. The slides were washed several times in PBS, mounted in Vectashield mounting medium with DAPI (Vector Laboratories), and visualized under an inverted fluorescence or light microscope. The following monoclonal (mAbs) and polyclonal antibodies (pAbs) were used: mouse anti-human HRP-conjugated α-SMA mAb (1:50, clone 1A4; DakoCytomation), rabbit anti–6-histidine tag pAb (1:400, clone NB600-318; Novus Biologicals), rabbit antimyeloperoxidase pAb (1:300, DakoCytomation), rat anti-F4/80 mAb (1:50, Caltag Laboratories), goat anti-CTGF/CCN2 pAb (1:25, clone L-20/sc-14939; Santa Cruz Biotechnology), and mouse anti-human decorin mAb (30 μg/mL, clone MAB143; R&D Systems).

Sandwich ELISA for Quantitation of Decorins. The recombinant decorins (100 μg) were injected into the blood stream via the tail vein and the blood collected at varying timepoints using 0.4% sodium citrate as an anticoagulant. Plasma was separated from cells by centrifugation at 5,000 *g* for 10 min. Wells of plastic microtiter plates were coated with monoclonal anti-human decorin antibody (2 μg/mL, clone MAB1432, R&D Systems) overnight at room temperature. Before the assay, the plates were washed four times with 0.05% Tween in PBS and blocked with 1% BSA in PBS. Dilutions of plasma were then incubated in the wells for 2 h in blocking solution. Nonbound plasma proteins were washed away with 0.05% Tween in PBS. Bound decorin was detected with biotinylated monoclonal anti-human decorin antibody (0.5 μg/mL, clone BAM1431; R&D Systems) for 2 h. After washing, streptavidin-conjugated horseradish peroxidase (Vector Laboratories) was added to the wells and incubated for 30 min at room temperature. The plate was washed again with PBS and HRP substrate (SIGMAFAST OPD; Sigma-Aldrich) was added. The reaction was stopped by addition of 2 M H_2SO_4, and the absorbance was read at 490 nm with an ELISA reader (Wallac).

Real-Time PCR. Mice with 5-d-old skin wounds were anesthetized and perfused through the heart with 25 mL of ice-cold PBS, after which the granulation/wound tissue was excised under an operating microscope. Approximately 20–30 mg of tissue was treated with RNAlater (Ambion) to preserve RNA. The tissue samples were immersed in the TRIzol reagent (Invitrogen), homogenized using MagNA Lyser (Roche Diagnostics), and prepared for RT-PCR as described (12). RT-PCR was performed using an Mx3000p instrument (Stratagene) by following the procedures as described in the RTProfiler PCR Array user manual (extracellular matrix and adhesion molecules PCR array, PAMM-013; SABiosciences). Replicate analysis consisted of four pools of RNA. Each pool of RNA was isolated from two wounds in two different animals ($n = 8$ per group).

1. Pilch J, et al. (2006) Peptides selected for binding to clotted plasma accumulate in tumor stroma and wounds. *Proc Natl Acad Sci USA* 103:2800–2804.
2. Krusius T, Ruoslahti E (1986) Primary structure of an extracellular matrix proteoglycan core protein deduced from cloned cDNA. *Proc Natl Acad Sci USA* 83:7683–7687.
3. Sheffield WP, Eltringham-Smith LJ, Gataiance S, Bhakta V (2009) A long-lasting, plasmin-activatable thrombin inhibitor aids clot lysis *in vitro* and does not promote bleeding *in vivo*. *Thromb Haemost* 101:867–877.
4. Carrino DA, et al. (2003) Age-related changes in the proteoglycans of human skin. Specific cleavage of decorin to yield a major catabolic fragment in adult skin. *J Biol Chem* 278:17566–17572.
5. Carrino DA, et al. (2010) Age-related differences in human skin proteoglycans. *Glygobiol*, 10.1093/glycob/cwq162.
6. Carrino DA, Sorrell JM, Caplan AI (2000) Age-related changes in the proteoglycans of human skin. *Arch Biochem Biophys* 373:91–101.
7. Esko JD, Stewart TE, Taylor WH (1985) Animal cell mutants defective in glycosaminoglycan biosynthesis. *Proc Natl Acad Sci USA* 82:3197–3201.
8. Yamaguchi Y, Mann DM, Ruoslahti E (1990) Negative regulation of transforming growth factor-β by the proteoglycan decorin. *Nature* 346:281–284.
9. Yamaguchi Y, Ruoslahti E (1988) Expression of human proteoglycan in Chinese hamster ovary cells inhibits cell proliferation. *Nature* 336:244–246.
10. Järvinen TAH, Ruoslahti E (2007) Molecular changes in the vasculature of injured tissues. *Am J Pathol* 171:702–711.
11. Krajewska M, et al. (2009) Image analysis algorithms for immunohistochemical assessment of cell death events and fibrosis in tissue sections. *J Histochem Cytochem* 57:649–663.
12. Galang CK, Muller WJ, Foos G, Oshima RG, Hauser CA (2004) Changes in the expression of many Ets family transcription factors and of potential target genes in normal mammary tissue and tumors. *J Biol Chem* 279:11281–11292.

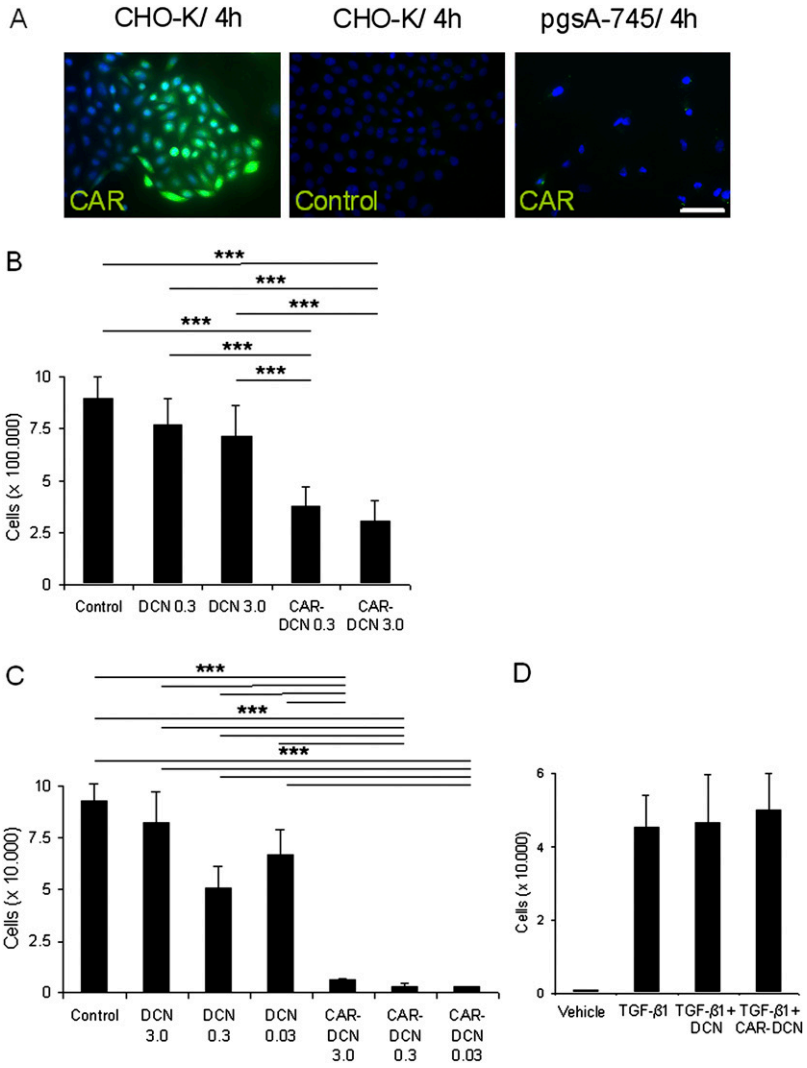

Fig. S1. The CAR peptide binding and proliferation of CHO-K and pgsA-745 cells in the presence of decorins. (*A*) Fluorescein-conjugated peptides were incubated at 5 μmol/L concentration with CHO-K and pgsA-745 cells for 4 h. The cells were washed, fixed, stained with the nuclear stain DAPI (blue), and examined for green fluorescence from the labeled peptides. The CAR peptide produces strong green fluorescence in the CHO-K cells (*Left*), but not in mutant pgsA-745 cells, which lack the receptor for CAR (10) (*Right*). A control peptide (10) gives no detectable cellular fluorescence (Scale bar, 50 μm.) (*B*) CHO-K cells were grown in media supplemented with dialyzed serum, which induces autocrine TGF-β production (9), and decorins as indicated (μg/mL) for 5 d. (*C*) CHO-K and (*D*) pgsA-745 cells were grown in serum-free media in the presence of TGF-β1 (7.5 ng/mL) and decorins (0.3 μg/mL or as indicated in *C*) for 4 d. Error bars represent mean ± SD. (*B*) CAR–decorin is more active than 10-fold higher dose of decorin in inhibiting the proliferation of CHO-K cells when grown in media supplemented with dialyzed serum. (*C*) CAR–decorin inhibits TGF-β1–driven cell proliferation more potently than 100-fold higher dose of nonmodified decorin in CHO-K cells. (*D*) CAR–decorin does not inhibit TGF-β1–driven cell proliferation when the receptor for CAR peptide is missing in the pgsA-745 cells (10). (*B* and *C*, $***P \leq 0.001$. *C*, NS. ANOVA).

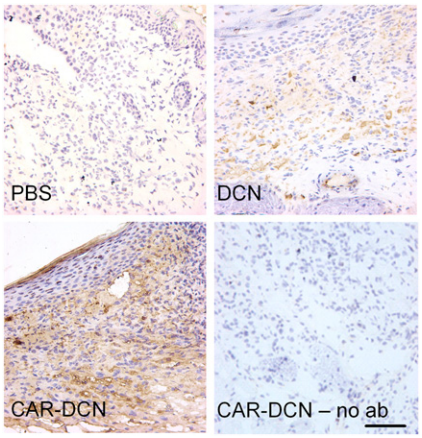

Fig. S2. Accumulation of peptide-guided decorin in wound tissue. Mice with full thickness skin wounds received daily i.v. injections of His-tagged proteins from day 3 to day 5 after the wounding. Six hours after the last injection on day 5, tissues were collected, and the presence of decorin in the tissues was determined with anti–6-histidine tag antibody (brown). The wounds of mice injected with nontargeted decorin (DCN) were weakly positive for decorin staining, whereas strong staining was observed throughout the granulation tissue of the CAR–DCN wounds. No staining was seen in wound tissue when class-matched mouse IgG was substituted for the anti–6-histidine tag antibody (no ab) (Scale bar, 80 μm.)

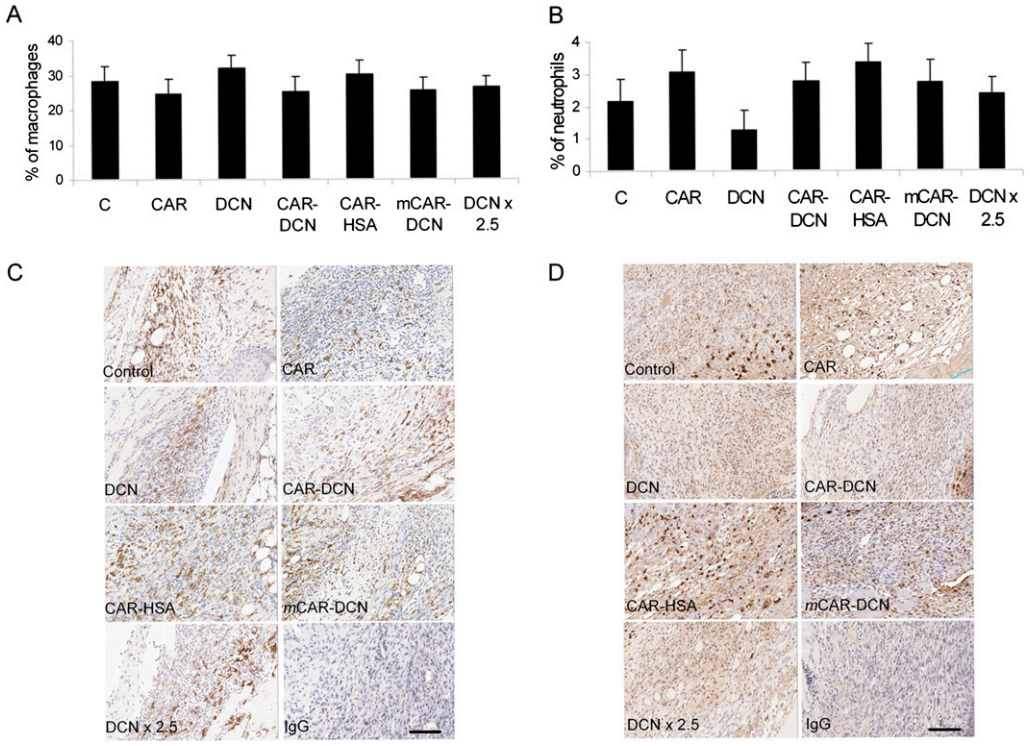

Fig. S3. Inflammatory cells in the wounds treated with decorin. The number of (*A*) macrophages and (*B*) neutrophils was determined by immunohistochemistry in wounds produced and treated as described in Fig. S2. Statistical significance was examined with ANOVA; no statistical differences were detected. The results are expressed as mean ± SD for eight wounds analyzed. Representative sections from wounds collected on day 5 after wounding are shown for macrophages (*C*) and for neutrophils (*D*). A wound from a decorin-treated mouse was stained with class-matched mouse IgG as a specificity control (IgG). The treatments did not affect the numbers of macrophages and neutrophils. (Scale bar, 100 μm.)

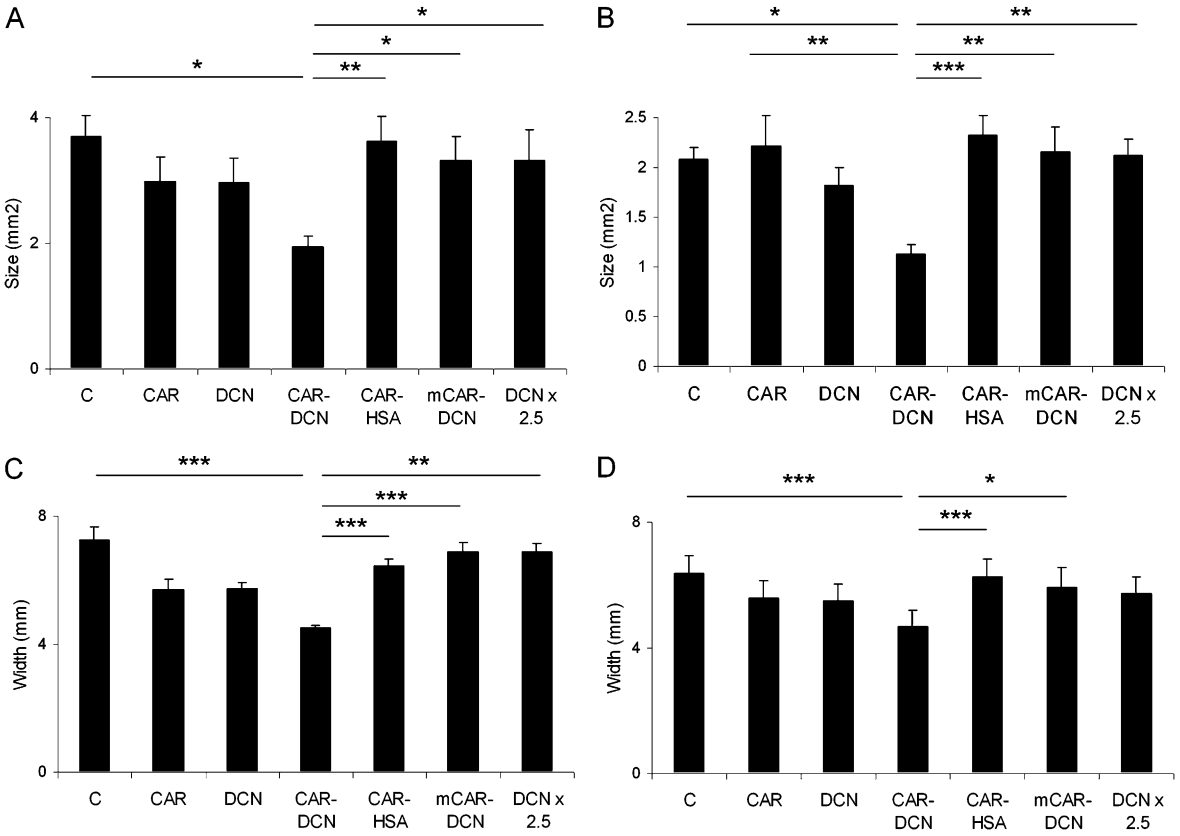

Fig. S4. Reduction in granulation tissue formation, scar formation, and wound length during wound healing in mice treated with CAR–decorin. Mice with full thickness skin wounds received daily i.v. injection as indicated from day 3 after the wounding until death. The area of granulation tissue/scar was quantified (*A*) at day 10 and (*B*) at day 14 simultaneously with quantification of the length (diameter) of hyperproliferative epidermis (*C*, day 10 and *D*, day 14) by examining two microscopic sections from each wound and expressed as the average of the two values. There were six (day 10) and seven animals (day 14), each with four wounds, in every treatment group. $*P < 0.05$, $**P \leq 0.01$, $***P \leq 0.001$, ANOVA. The results are expressed as mean ± SEM, $n = 24$ at day 10 and $n = 28$ at day 14.

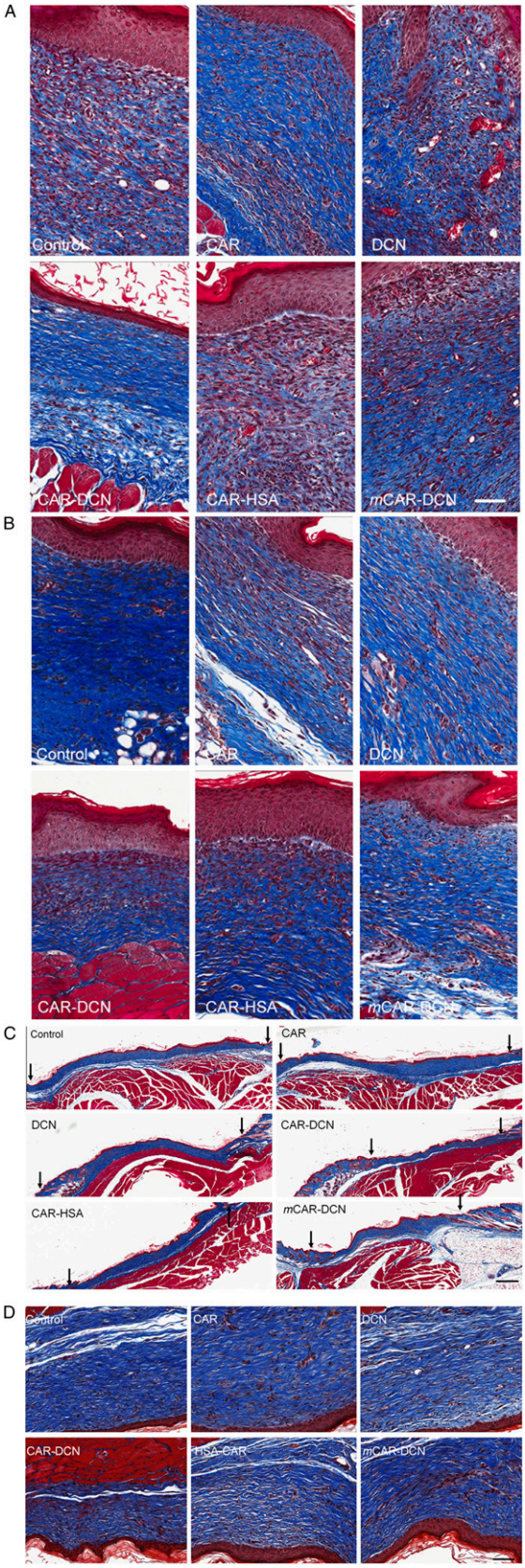

Fig. S5. Reduction in granulation tissue formation during wound healing in mice treated with CAR–decorin. Mice with full thickness skin wounds received daily i.v. injection as indicated from day 3 after the wounding until sacrifice. Representative microscopic fields from the wounds of animals on days 10 (*A*) and 14 (*B*) are shown. The images show a significant reduction in the production of hypertrophic granulation tissue/scar in wounds treated with CAR–DCN compared with the other treatment groups. (Scale bars, 80 μm.) (*C* and *D*) Representative microscopic fields from the wounds of animals on day 21. Arrows indicate edges of the wound in *C*. Wounds in the CAR–DCN group have the thickness of normal skin, whereas hypertrophic scar tissue is seen in the dermal part of the wounds in the other treatment groups (*D*). [Scale bars, (*C*) 400 μm and (*D*) 80 μm.]

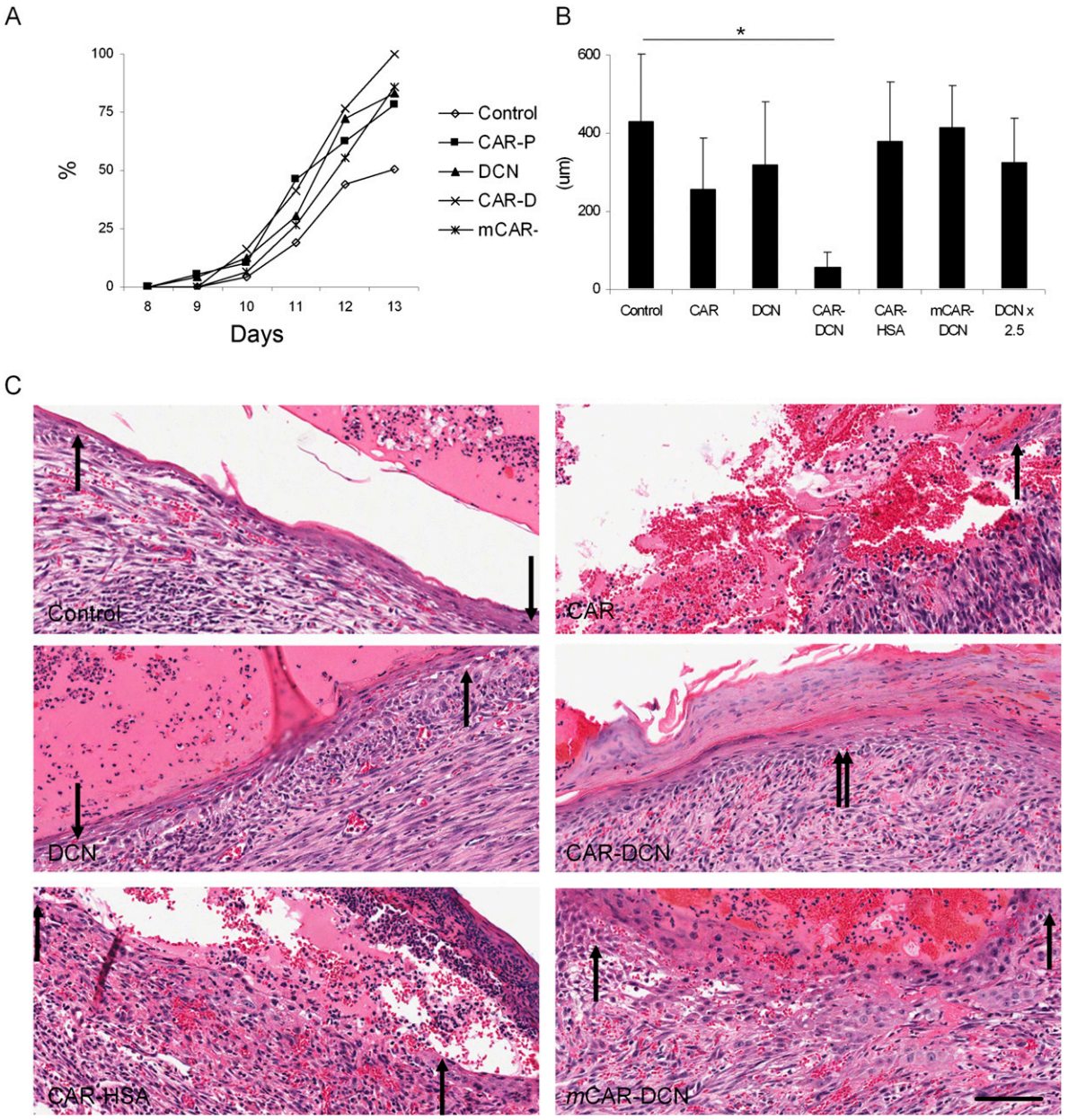

Fig. S6. Wound closure in treated animals. (*A*) The wounds of animals treated as in Fig. S4 were examined and photographed daily. Wound closure was recorded and expressed as percentage of completely closed wounds (complete reepithelialization). (*B*) The gap in the epidermis was quantified on day 10 by examining two microscopic sections from each wound and expressed as the average of the two values. (*C*) Representative microscopic fields from the wounds of animals on day 10 are shown. The images show accelerated wound closure (reepithelialization) in wounds treated with CAR–DCN compared with the other treatment groups. The arrows indicate tips of epithelial tongues in the wounds. (Scale bar, 30 μm.) Statistical significance was examined using the χ^2 test. $n = 80$ at day 10, $n = 56$ at days 11–13 (*A*), and for the histological analysis $n = 24$.

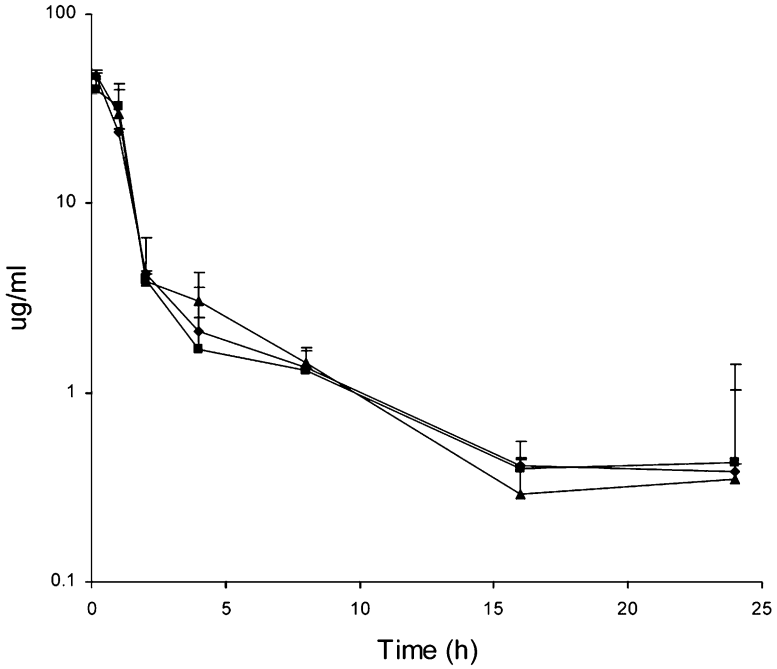

Fig. S7. Half-life of recombinant decorins in circulation. Mice received i.v. injections of recombinant decorins (100 μg). The injected decorins were allowed to circulate for various periods of time from 15 min to 24 h, blood was collected, and decorin concentration in plasma was determined by sandwich ELISA. Native decorin (DCN; ■), CAR–DCN (◇), and *m*CAR–DCN (▲). All have similar half-lives in the circulation of normal mice without wounds. $n = 2–3$ for each timepoint. No statistical differences were detected by ANOVA.

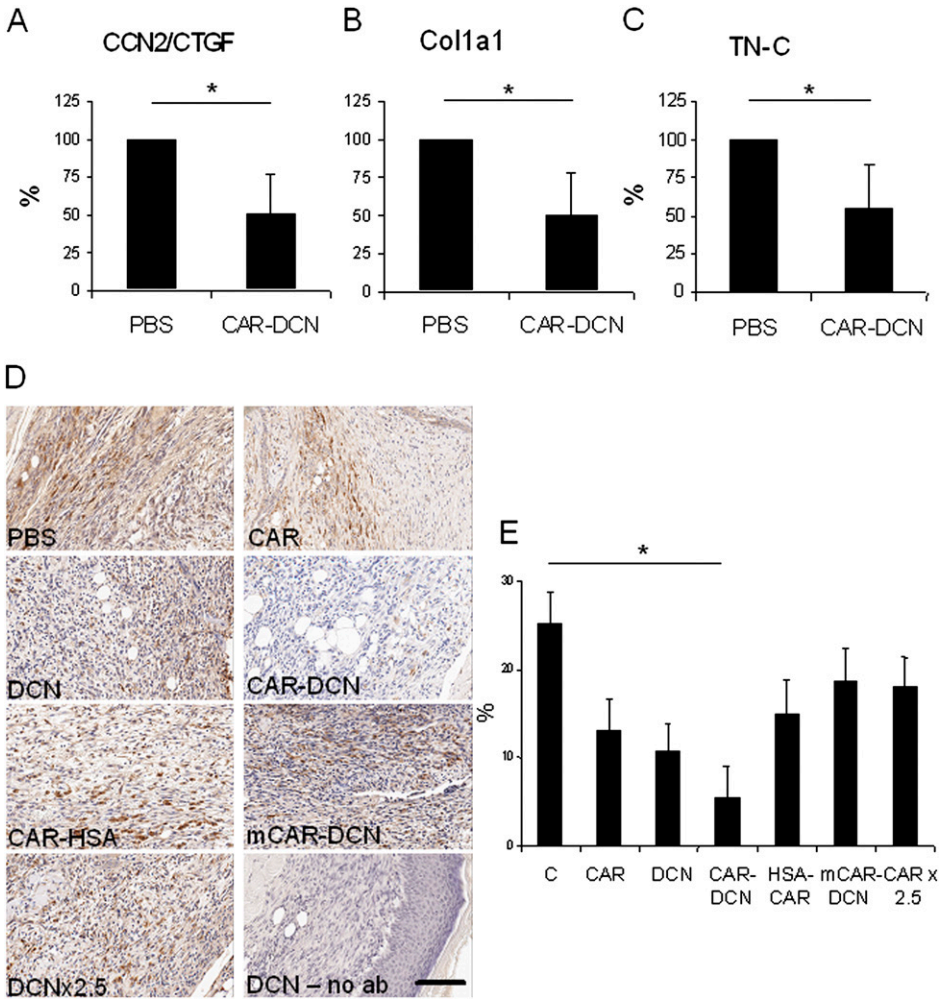

Fig. S8. Effect of CAR-targeted decorin on mRNA and protein expression of TGF-β–regulated genes in skin wounds. The expression of mRNA for connective tissue growth factor CCN2/CTGF (*A*), collagen I α1 (*B*), and tenascin-C (*C*). (*D*) Expression of CCN2/CTGF protein on day 5 in wounds treated with decorins. Mice with full thickness skin wounds received daily i.v. injections as indicated from day 3 to day 5 after the wounding. The wounds were harvested on day 5 for qPCR and immunohistochemistry. The mRNA levels of the PBS/BSA control group were assigned the value 100%. CCN2/CTGF protein was determined from histological slides with antibody staining, and the area of positive staining was quantified with image software (*E*). Error bars represent mean ± SD from four pools of RNA isolated from two wounds in each of two different animals in the mRNA plots and mean ± SEM from eight wounds are shown for CCN2/CTGF expression. Statistical significance was examined using the (*A*–*C*) two-tailed *t* test and (*E*) ANOVA, $*P < 0.05$. (Scale bars, 100 μm.)

Table S1. Accelerated wound closure by targeted decorin

	Day 11	Day 12	Day 13
CAR	<0.05	NS	<0.05
DCN	NS	<0.05	<0.01
CAR–DCN	<0.01	<0.001	<0.001
*m*CAR–DCN	NS	NS	<0.001

The wounds of animals treated as in Fig. S4 were examined and photographed daily. Wound closure was recorded and expressed as percentage of completely closed wounds (complete reepithelialization) and compared with untreated wounds. χ^2 test; $n = 80$ at day 10; $n = 56$ at days 11–13.